Radiology: Cardiothoracic Imaging

ORIGINAL RESEARCH

Chest CT Severity Score: An Imaging Tool for Assessing Severe COVID-19

*Ran Yang** • *Xiang Li** • *Huan Liu* • *Yanling Zhen* • *Xianxiang Zhang* • *Qiuxia Xiong* • *Yong Luo* • *Cailiang Gao* • *Wenbing Zeng, MS*

From the Department of Radiology, Chongqing University Three Gorges Hospital, Chongqing 404000, China (R.Y., X.L., X.Z., Q.X., Y.L., C.G., W.Z.); Department of Radiology, Chongqing Three Gorges Central Hospital, Chongqing, China (R.Y., X.L., X.Z., Q.X., Y.L., C.G., W.Z.); GE Healthcare, Shanghai, China (H.L.); and Department of Radiology, Affiliated Hospital of North Sichuan Medical College, Sichuan, China (Y.Z.). Received February 14, 2020; revision requested February 21; revision received March 18; accepted March 19. **Address correspondence to** W.Z. (e-mail: *zeng_wenbing@163.com*).

Project No. 2020CDJYGRH-YJ03 supported by the Fundamental Research Funds for the Central Universities.

*R.Y. and X.L. contributed equally to this work.

Conflicts of interest are listed at the end of this article.

Radiology: Cardiothoracic Imaging 2020; 2(2):e200047 • https://doi.org/10.1148/ryct.2020200047 • Content code: CH

Purpose: To evaluate the value of chest CT severity score (CT-SS) in differentiating clinical forms of coronavirus disease 2019 (COVID-19).

Materials and Methods: A total of 102 patients with COVID-19 confirmed by a positive result from real-time reverse transcription polymerase chain reaction on throat swabs who underwent chest CT (53 men and 49 women, 15–79 years old, 84 cases with mild and 18 cases with severe disease) were included in the study. The CT-SS was defined by summing up individual scores from 20 lung regions; scores of 0, 1, and 2 were respectively assigned for each region if parenchymal opacification involved 0%, less than 50%, or equal to or more than 50% of each region (theoretic range of CT-SS from 0 to 40). The clinical and laboratory data were collected, and patients were clinically subdivided according to disease severity according to the Chinese National Health Commission guidelines.

Results: The posterior segment of upper lobe (left, 68 of 102; right, 68 of 102), superior segment of lower lobe (left, 79 of 102; right, 79 of 102), lateral basal segment (left, 79 of 102; right, 70 of 102), and posterior basal segment of lower lobe (left, 81 of 102; right, 83 of 102) were the most frequently involved sites in COVID-19. Lung opacification mainly involved the lower lobes, in comparison with middle-upper lobes. No significant differences in distribution of the disease were seen between right and left lungs. The individual scores in each lung and the total CT-SS were higher in severe COVID-19 when compared with mild cases ($P < .05$). The optimal CT-SS threshold for identifying severe COVID-19 was 19.5 (area under curve = 0.892), with 83.3% sensitivity and 94% specificity.

Conclusion: The CT-SS could be used to evaluate the severity of pulmonary involvement quickly and objectively in patients with COVID-19.

Since December 2019, a cluster of cases with unknown pneumonia with similar clinical manifestations suggesting viral pneumonia appeared in Wuhan city, Hubei Province, China. A new type of coronavirus was isolated from the lower respiratory tract samples, named severe acute respiratory syndrome coronavirus-2 (SARS-CoV-2) by the International Committee on Taxonomy of Viruses (1). The disease it causes was named coronavirus disease 2019 (COVID-19) by the World Health Organization on February 11, 2020 (2). SARS-CoV-2 belongs to β-coronavirus, which is a typical RNA virus. It is generally round or oval shaped, with a diameter of 60 to 140 nm under the electron microscope. Its outer membrane had unique spikes, about 9 to 12 nm, similar to the solar corona (3). The study found that the SARS-CoV-2 shares 92% homology with the bat coronavirus sequence RaTG3, which suggests a zoonotic origin for this outbreak (4). SARS-CoV-2 can spread from person to person (5), and COVID-19 has been declared a pandemic disease. The common clinical symptoms of patients with COVID-19 are fever, cough, dyspnea, and fatigue, which are similar to those of severe acute respiratory syndrome coronavirus (SARS-CoV) and Middle East respiratory syndrome coronavirus (6,7). Severe cases can lead to acute respiratory distress syndrome or even death. According to the severity of the patient's condition, the treatment differs. Patients with mild disease receive antivirals, symptomatic support, and oxygen therapy. However, patients with severe symptoms need to be admitted to an intensive care unit as soon as possible.

At present, the diagnosis of COVID-19 depends on real-time reverse transcription polymerase chain reaction or next-generation sequencing (8). At imaging, CT manifestations resemble those seen in viral pneumonias (9), with multifocal ground-glass opacities and consolidation in a peripheral distribution being the most common findings (10,11). Although these findings lack specificity for a COVID-19 diagnosis on imaging grounds, we hypothesize that CT could be used to provide objective assessment about the extension of the lung opacities, which could be used as an imaging surrogate for disease burden. The main purpose of our study was to evaluate the performance and interreader concordance of a semiquantitative CT severity score (CT-SS) designed to identify the severity of COVID-19. If feasible, such an approach could expedite the identification and management of patients with severe disease in specific instances where a fast triage method is needed.

Abbreviations

COVID-19 = coronavirus disease 2019, CT-SS = CT severity score, ICC = intraclass correlation coefficient, ROC = receiver operating characteristic, SARS-CoV-2 = severe acute respiratory syndrome coronavirus 2

Summary

The chest CT severity score could be used to rapidly identify patients with severe forms of coronavirus disease 2019.

Key Points

- The dominant distribution of coronavirus disease 2019 pneumonia is bilateral and posterior.
- The proposed pulmonary inflammation load score was higher in patients with severe coronavirus disease 2019 than in those with mild disease.
- The optimal inflammation load score threshold for identifying patients with severe infection was 19.5, with 83.3% sensitivity and 94% specificity.

Materials and Methods

Patients and Groups

This study was approved by the Ethics Committee of Chongqing Three Gorges Central Hospital. We retrospectively studied the patients who were diagnosed with COVID-19 from January 21 to February 5, 2020, in our hospital. According to our hospital protocol, all patients suspected of having COVID-19 routinely underwent noncontrast CT examinations and were admitted in hospital for isolation and observation. CT was chosen over chest radiography on the basis of the assumption that the former is more sensitive to detect lung opacities.

A total of 102 patients with COVID-19 were confirmed by using a real-time reverse transcription polymerase chain reaction throat swab (12). Patients with lung malignancy, a history of lobectomy, tuberculosis, or atelectasis were excluded from this study. According to the "Diagnosis and Treatment Program of Pneumonia of New Coronavirus Infection (Trial Fifth Edition)" (13) recommended by China's National Health Commission on February 5, 2020, patients with COVID-19 are classified as having minimal, common, severe, and critical disease. Patients with minimal disease have subtle clinical symptoms and no lung opacities on chest imaging and have been excluded from further analyses in this study. Common cases have symptoms such as fever and respiratory tract infection and chest images showing lung opacities. Severe cases should meet any of the following criteria: *(a)* respiratory distress, respiratory rate $\geq$ 30 beats per minute; *(b)* resting blood oxygen saturation $\leq$ 93%; or *(c)* partial pressure of arterial blood oxygen (PaO2) or oxygen concentration (FiO2) $\leq$ 300 mm Hg. Critical patients need to meet one of the following conditions: *(a)* respiratory failure and need for mechanical ventilation; *(b)* shock; and *(c)* other organ failure needing intensive care unit monitoring treatment.

For the purposes of this study, common cases were included in the mild disease group, whereas severe and critical cases were merged into the severe disease group because of the small number of cases in the latter category (n = 3).

Chest CT-SS Assessment

We developed a chest CT-SS for assessing COVID-19 burden on the initial scan obtained at admission. This score uses lung opacification as a surrogate for extension of the disease in the lungs. The CT-SS is an adaptation of a method previously used to describe ground-glass opacity, interstitial opacity, and air trapping, which was correlated with clinical and laboratory parameters in patients after SARS (14). According to the anatomic structure, the 18 segments of both lungs were divided into 20 regions, in which the posterior apical segment of the left upper lobe was subdivided into apical and posterior segmental regions, whereas the anteromedial basal segment of the left lower lobe was subdivided into anterior and basal segmental regions. The lung opacities in all of the 20 lung regions were subjectively evaluated on chest CT images using a system attributing scores of 0, 1, and 2 if parenchymal opacification involved 0%, less than 50%, or equal to or more than 50% of each region, respectively. The CT-SS was defined as the sum of the individual scores in the 20 lung segment regions, which may range from 0 to 40 points.

All CT images were independently reviewed by two chest radiologists with more than 10 years of experience, blinded to the clinical data and laboratory indicators, in a standard clinical picture archiving and diagnostic system workstation. All thin-section CT images were reviewed at a window width and level of 1000 to 2000 HU and −700 to −500 HU, respectively, for lung parenchyma.

Chest CT Scan

Chest CT imaging was performed using a 16-detector CT scanner (Emotion; Siemens). All patients were examined in the supine position. CT images were then acquired during a single inspiratory breath-hold. The scanning range was from the apex of the lung to the costophrenic angle. CT scan parameters were as follows: x-ray tube parameters 120 kVp, 350 mAs; rotation time 0.5 second; pitch 1.0; section thickness 5 mm; intersection space 5 mm; additional reconstruction with a sharp convolution kernel; and a slice thickness of 1.5 mm.

Statistical Analysis

Statistical analysis was performed using R (version 3.5.1). $P <$ .05 was regarded to demonstrate statistical significance. Quantitative data were expressed as mean $\pm$ standard deviation or median and interquartile range. The weighted kappa coefficient was used to compare the consistency of two observers in each lung segment. Interrater reliability was evaluated using intraclass correlation coefficient (ICCs) for continuous variables. (ICCs were classified as follows: no agreement, 0–0.2; weak agreement, 0.21–0.4; moderate agreement, 0.41–0.60; good agreement, 0.61–0.80; and excellent agreement, 0.81–1.0). All measurements were assessed with normality tests. A χ^2 or Fisher exact test was used to compare the scores of each lung segment between the mild and severe groups. A Wilcoxon rank sum test was used to compare the difference of left lung, right lung, and total score between the mild group and the severe group, and the Wilcoxon matched-pairs signed-rank test was

Table 1: Demographic and Clinical Data of 102 Patients with COVID-19 Pneumonia

Variable	Mild (n = 84)	Severe (n = 18)	Statistics	P Value
Sex			0.113	.737
Male	43 (51.19)	10 (55.56)		
Female	41 (48.81)	8 (44.44)		
Age (y)			−2.946	.004*
Mean ± SD	43.70 ± 11.71	52.83 ± 12.96		
Range	15–78	31–79		
Cough			1.71	.191
No	27 (32.14)	3 (16.67)		
Yes	57 (67.86)	15 (83.33)		
Expectoration			1.105	.293
No	79 (94.05)	15 (83.33)		
Yes	5 (5.95)	3 (16.67)		
Fever			0.053	.817
No	13 (15.48)	3 (16.67)		
Yes	71 (84.52)	15 (83.33)		
Temperature	37.50 (36.90–38.00)	37.80 (37.29–38.00)	−0.733	.464
Mechanical ventilation			Inf	.005*
No	84 (100.00)	15 (83.33)		
Yes	0 (0.00)	3 (16.67)		
Time of onset (days)	6.00 (4.00–9.00)	9.00 (7.00–12.05)	−2.971	.003*
RR (beats/min; 12–20)	20.00 (19.00–20.00)	25.00 (20.00–33.25)	−4.736	<.001*
SO_2 (≥ 0.95)	0.97 (0.96–0.98)	0.92 (0.88–0.93)	6.276	<.001*
WBC (10^9/L; 3.5–9.5)	5.00 (4.00–6.30)	5.20 (3.50–6.53)	0.075	.941
NEU% (0.45–0.75), mean ± SD	0.66 ± 0.11	0.79 ± 0.10	−4.422	<.001*
LYM% (0.20–0.50)	0.25 (0.19–0.31)	0.15 (0.09–0.22)	4.17	<.001*
NEU (10^9/L; 1.8–6.3)	3.40 (2.42–4.17)	3.35 (2.45–5.25)	−0.584	.559
LYM (10^9/L; 1.1–3.2)	1.21 (0.90–1.50)	0.68 (0.46–0.96)	4.45	<.001*
HSCRP (mg/L; 0–11)	11.29 (2.71–37.46)	107.91 (47.41–135.93)	−5.267	<.001*
PCT (ng/mL; < 0.046)	0.04 (0.03–0.07)	0.09 (0.06–0.21)	−4.499	<.001*

Note.—Data are presented as median and interquartile range and numbers with percentages in parentheses, unless otherwise specified. HSCRP = hypersensitive C-reactive protein; LYM = lymphocyte; NEU = neutrophil, PCT = procalcitonin, RR = respiratory rate; SD = standard deviation, SO_2 = blood oxygen saturation; WBC = white blood cell.
* P values less than .05 were considered statistically significant.

used to compare the difference of scores between lower lung and middle-upper lung, left lung, and right lung. A receiver operating characteristic (ROC) curve analysis was performed to calculate the threshold, specificity, sensitivity, and accuracy for discriminating the mild from the severe COVID-19 group.

Results

Clinical and Laboratory Findings

Table 1 shows the demographic and clinical data of 102 patients at the time of admission. A total of 102 patients were included in this study, 84 in the mild group and 18 in the severe group, with respective average ages of 43.70 and 52.83 years (P = .004) and male-to-female ratios of 43:41 and 10:8. The average body temperature of the patients was 37.5°C (mild group) and 37.8°C (severe group), and no statistical difference was found (P = .464). The most common clinical symptoms were cough (72 of 102, 70.59%) and fever (86 of 102, 84.31%). The time from onset of symptoms and respiratory rate in the severe group were higher than those of the mild group, and the blood oxygen saturation was decreased in the former group (P < .05). Only three patients in the severe group needed mechanical ventilation, whereas none in the mild group needed ventilatory support. The percentage and absolute lymphocyte counts were lower in the severe group (P < .001). The percentage of neutrophils and serum concentrations of hypersensitive C-reactive protein and procalcitonin were higher in the severe group than the mild group (P < .001).

Imaging Findings

The interreader ICCs for CT-SS were excellent (n = 102, ICC_{median}=0.925, ICC_{mean}=0.936). The scores provided by one of the two readers were randomly chosen for further analyses. Figure 1 displays the total number of patients with lung opacities

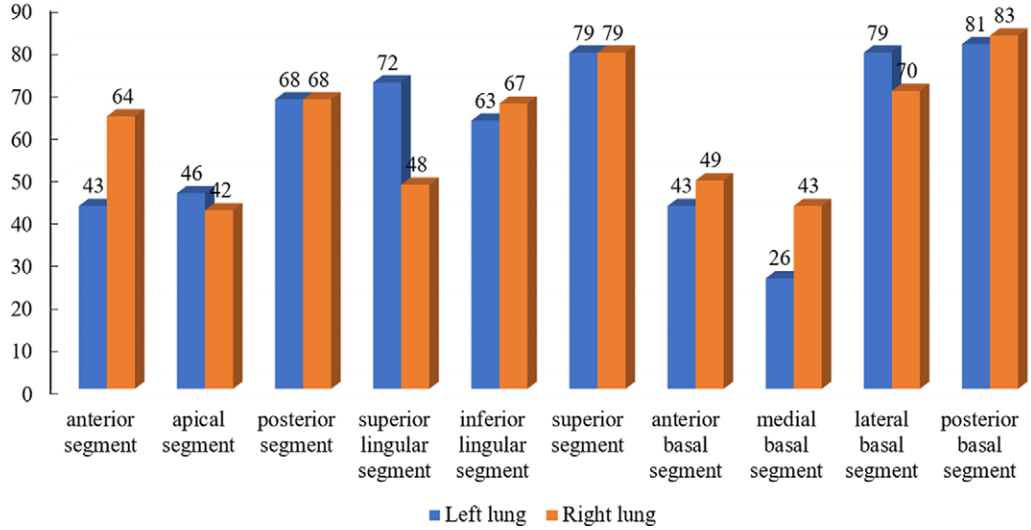

Figure 1: Number of patients involved in each lung segment.

Table 2: Comparison of Scores of Each Lung Segment between the Two Groups

Variable	Sample	Mild (n = 84)	Severe (n = 18)	P Value	Kappa
Anterior segment (L)				.002	0.648
0	59	53 (63.10)	6 (33.33)		
1	41	31 (36.90)	10 (55.56)		
2	2	0 (0.00)	2 (11.11)		
Apical segment (L)				<.001	0.776
0	56	52 (61.90)	4 (22.22)		
1	44	32 (38.10)	12 (66.67)		
2	2	0 (0.00)	2 (11.11)		
Posterior segment (L)				<.001	0.782
0	34	32 (38.10)	2 (11.11)		
1	54	46 (54.76)	8 (44.44)		
2	14	6 (7.14)	8 (44.44)		
Superior lingular segment (L)				.002	0.829
0	30	29 (34.52)	1 (5.56)		
1	65	52 (61.90)	13 (72.22)		
2	7	3 (3.57)	4 (22.22)		
Inferior lingular segment (L)				<.001	0.798
0	39	38 (45.24)	1 (5.56)		
1	51	42 (50.00)	9 (50.00)		
2	12	4 (4.76)	8 (44.44)		
Superior segment (L)				<.001	0.883
0	23	22 (26.19)	1 (5.56)		
1	56	51 (60.71)	5 (27.78)		
2	23	11 (13.10)	12 (66.67)		
Anterior basal segment (L)				<.001	0.687
0	59	55 (65.48)	4 (22.22)		
1	37	29 (34.52)	8 (44.44)		
2	6	0 (0.00)	6 (33.33)		
Medial basal segment (L)				<.001	0.799
0	76	69 (82.14)	7 (38.89)		
1	21	15 (17.86)	6 (33.33)		
2	5	0 (0.00)	5 (27.78)		

Table 2 (continues)

Table 2 (continued): Comparison of Scores of Each Lung Segment between the Two Groups

Variable	Sample	Mild (n = 84)	Severe (n = 18)	P Value	Kappa
Lateral basal segment (L)				<.001	0.816
0	23	23 (27.38)	0 (0.00)		
1	68	58 (69.05)	10 (55.56)		
2	11	3 (3.57)	8 (44.44)		
Posterior basal segment (L)				<.001	0.807
0	21	21 (25.00)	0 (0.00)		
1	64	55 (65.48)	9 (50.00)		
2	17	8 (9.52)	9 (50.00)		
Anterior segment (R)				.006	0.757
0	38	36 (42.86)	2 (11.11)		
1	61	47 (55.95)	14 (77.78)		
2	3	1 (1.19)	2 (11.11)		
Apical segment (R)				.011	0.721
0	60	54 (64.29)	6 (33.33)		
1	39	29 (34.52)	10 (55.56)		
2	3	1 (1.19)	2 (11.11)		
Posterior segment (R)				<.001	0.878
0	34	31 (36.90)	3 (16.67)		
1	59	51 (60.71)	8 (44.44)		
2	9	2 (2.38)	7 (38.89)		
Medial segment (R)				<.001	0.891
0	54	50 (59.52)	4 (22.22)		
1	42	34 (40.48)	8 (44.44)		
2	6	0 (0.00)	6 (33.33)		
Lateral segment (R)				<.001	0.966
0	35	33 (39.29)	2 (11.11)		
1	56	47 (55.95)	9 (50.00)		
2	11	4 (4.76)	7 (38.89)		
Superior segment (R)				<.001	0.858
0	23	21 (25.00)	2 (11.11)		
1	63	58 (69.05)	5 (27.78)		
2	16	5 (5.95)	11 (61.11)		
Anterior basal segment (R)				<.001	0.770
0	53	49 (58.33)	4 (22.22)		
1	43	35 (41.67)	8 (44.44)		
2	6	0 (0.00)	6 (33.33)		
Medial basal segment (R)				<.001	0.793
0	59	55 (65.48)	4 (22.22)		
1	37	28 (33.33)	9 (50.00)		
2	6	1 (1.19)	5 (27.78)		
Lateral basal segment (R)				<.001	0.664
0	32	30 (35.71)	2 (11.11)		
1	58	50 (59.52)	8 (44.44)		
2	12	4 (4.76)	8 (44.44)		
Posterior basal segment (R)				.001	0.761
0	19	18 (21.43)	1 (5.56)		
1	61	54 (64.29)	7 (38.89)		
2	22	12 (14.29)	10 (55.56)		
Score of left lung	102	6.00 (3.00–8.00)	12.00 (9.00–14.00)	<.001	0.925*
Score of right lung	102	6.00 (3.45–8.00)	12.00 (9.00–16.05)	<.001	0.892*
Total score	102	13.00 (6.00–16.00)	23.50 (20.95–30.05)	<.001	0.990*

Note.—Data are presented as median and interquartile range and numbers with percentages in parentheses. L = left lung; R = right lung.
*ICC: intraclass correlation coefficient.

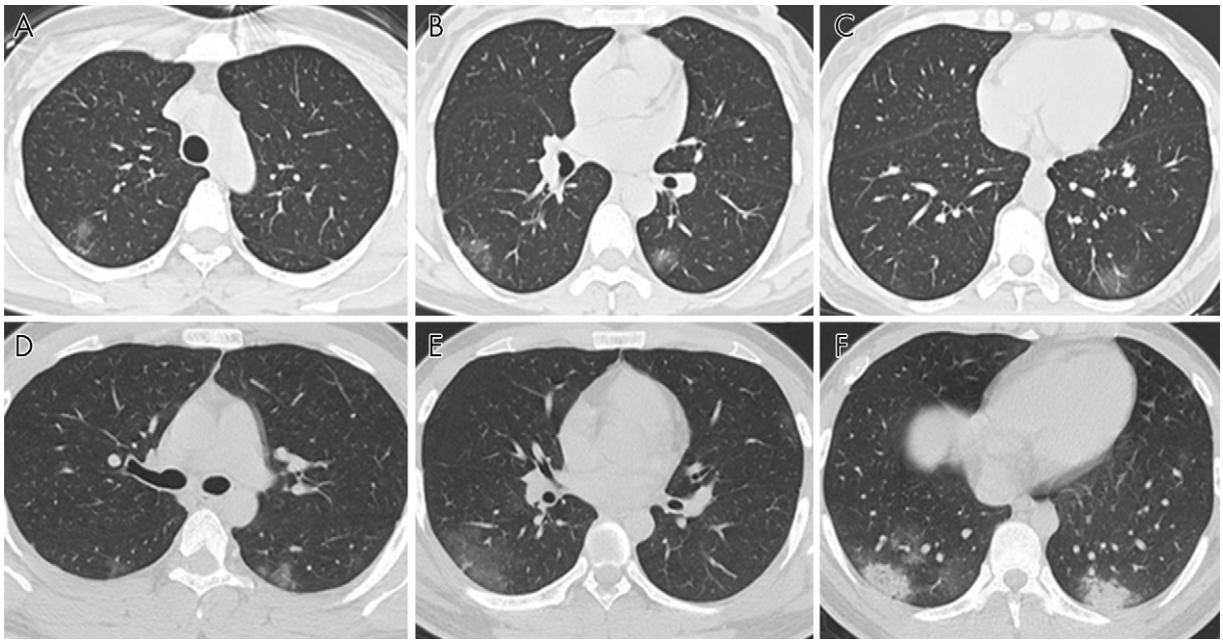

Figure 2: *A-C,* Noncontrast chest CT images in a 46-year-old woman with mild COVID-19 pneumonia. CT images show ground-glass opacities in the posterior segment of right upper lobe, superior segment of bilateral lungs, and posterior basal segment of right left lobe, and the CT-SS is 4. *D-F,* Noncontrast chest CT images in a 20-year-old man with mild COVID-19 pneumonia. CT images show ground-glass opacities and consolidation in multiple lung segments, and the CT-SS is 7.

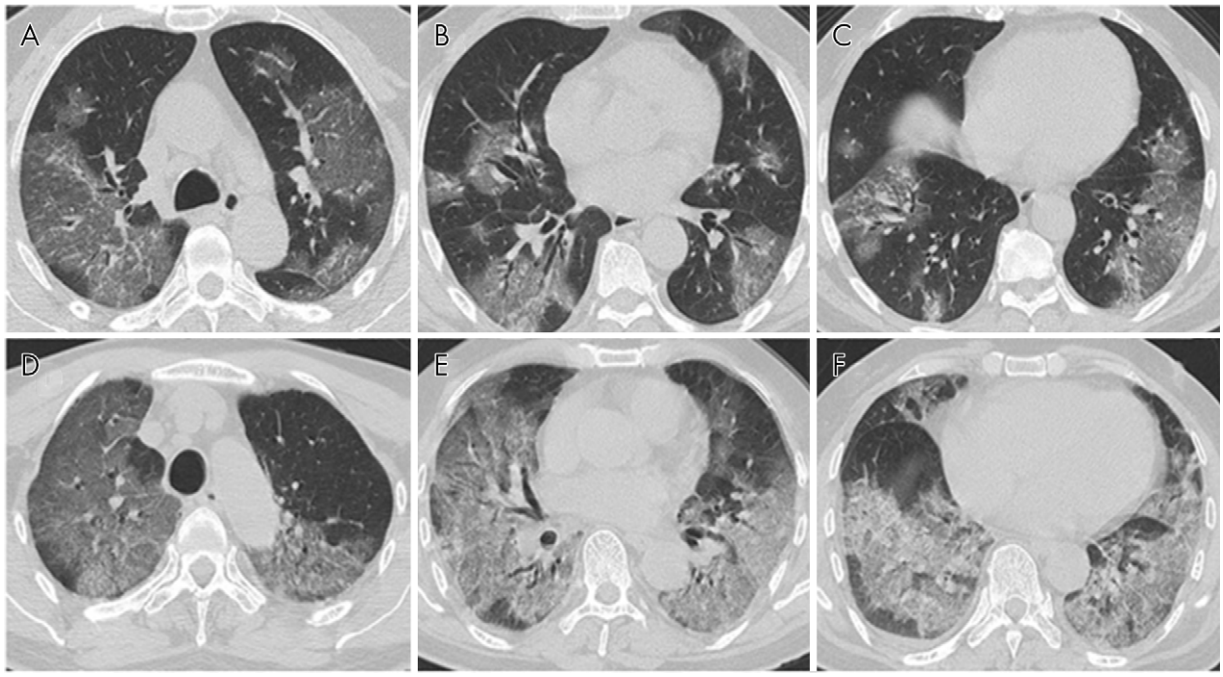

Figure 3: *A-C,* Noncontrast chest CT images in a 56-year-old man with severe COVID-19 pneumonia. CT images show multiple ground-glass opacities in multiple lung segments, and the CT-SS is 28. *D-F,* Noncontrast chest CT images in a 69-year-old man with severe COVID-19 pneumonia. CT images show multiple ground-glass opacities and septal thickening; the imaging manifestation is the so-called white lungs; the CT-SS is 35.

in each of the lung segments. Overall, the posterior segment of the upper lobes (left, 68 of 102 [66.7%]; right, 68 of 102 [66.7%]), the superior segment of the lower lobes (left, 79 of 102 [77.5%]; right, 79 of 102 [77.5%]), the lateral basal segments of the lower lobes (left, 79 of 102 [77.5%]; right, 70 of 102 [68.6%]), and the posterior basal segments of the lower lobes (left, 81 of 102 [79.4%]; right, 83 of 102 [81.4%]) are the most frequently involved sites in COVID-19. There were significant differences between the lung opacity scoring of the mild and severe groups in each lung region, $P < .05$ (Table 2). The left lung score was 6.0 (3.0, 8.0), right lung score was 6.0 (3.45, 8.0), and total CT-SS was 13.0 (6.0, 16.0) in the mild group, and the left lung score was 12.0 (9.0, 14.0), right lung score was 12.0 (9.0, 16.05), and total CT-SS was 23.5 (20.95,

Table 3: Comparison of Left Lung Score and Right Lung Score, Lower Lung Score, and Upper-Middle Lung Score

Variable	Left Lung	Right Lung	*P* Value	Middle-Upper Lung	Lower Lung	*P* Value
Mild (*n* = 84)	6.0 (3.0–8.0)	6.0 (3.45–8.0)	.583	6.0 (2.75–9.0)	7.0 (4.0–8.0)	.011*
Severe (*n* = 18)	12.0 (9.0–14.0)	12.0 (9.0–16.05)	.938	11.0 (10.0–3.5)	12.5 (9.25–16.5)	.038*

Note.—Data are presented as median and interquartile range. Wilcoxon matched-pairs signed-rank test was used.
**P* values less than .05 were considered statistically significant.

Table 4: Secondary CT Findings of 102 Patients with COVID-19

Variable	Mild (*n* = 84)	Severe (*n* = 18)	Total	*P* Value
Pleural effusions	0	7	7	.833
Lymphadenopathy	0	2	2	
Total	0	9	9	

Note.—Fisher exact test was used.

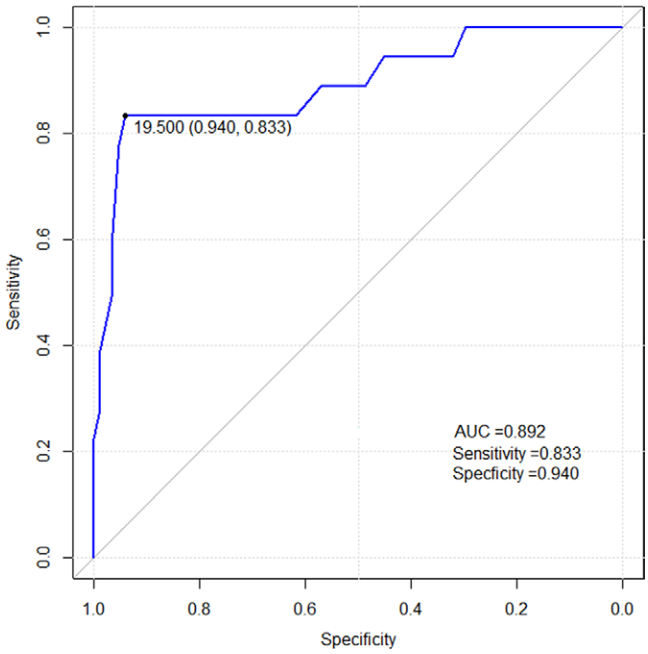

Figure 4: ROC curve for CT-SS.

30.05) in the severe group (Table 2, Figs 2, 3). The lower lobe scores were higher than the middle-upper lobe scores in each group. However, there were no significant differences between left and right lung scores (Table 3). Pleural effusions were found in seven cases and lymphadenopathy in two cases in the severe group, whereas pleural effusion and lymphadenopathy were not found in the mild group (Table 4).

ROC Curve for CT-SS

The ROC curve analysis for CT-SS is shown in Figure 4. The area under the ROC curve for discriminating patients in the mild and severe group was 0.892 (standard error, 0.05; 95% confidence interval: 0.814, 0.944), and the optimal CT-SS threshold for identifying severe patients was 19.5, with 83.3% sensitivity and 94% specificity. The number of patients with CT-SS equal to or greater than 19.5 was 15 in the severe group and five in the mild group, and the number of patients with CT-SS less than 19.5 was 3 and 79, respectively, resulting in a positive predictive value of 75.0% and a negative predictive value for severe disease of 96.3%.

Discussion

On January 30, 2020, the World Health Organization declared COVID-19 as the sixth public health emergency deserving international attention. COVID-19 is highly contagious and has spread worldwide. Strategies for disease containment and patient management heavily rely on disease diagnosis (3,15,16). However, COVID-19 testing has been challenged by limited laboratory facilities and inadequate supply of nucleic acid kits (17). Moreover, the lack of early abnormalities on chest radiographs can lead to a large number of false negatives (18). Thin-section chest CT is more sensitive than chest radiography, showing abnormal changes in the lung parenchyma in the early stages of disease (19,20). For these reasons, chest CT has become a forefront diagnostic method during the outbreak of COVID-19 in China (18).

The typical imaging manifestations of early COVID-19 are patchy, rounded, segmental or subsegmental ground-glass opacities with or without consolidation (20). Lesions are multiple and asymmetrically distributed and are more common in the peripheral areas (11,21,22). Some imaging findings of COVID-19 overlap with those of other RNA viral infection, such as respiratory syncytial virus and human parainfluenza virus (9,23). Song et al (24) retrospectively analyzed the chest CT images of 51 patients with COVID-19; the results showed that 82% of the patients had posterior lung involvement, which are closely matched with our observations. Noticeably, the dominant posterior distribution is similar to reports on SARS-CoV and Middle East respiratory syndrome coronavirus infection (25,26). In our study, we also found a slight predominance of opacities in the lower lobes when compared with the middle and upper lobes, without significant differences between the right and left lung, which was also consistent with previous analyses (27).

In this study, we devised a semiquantitative scoring method using the amount of lung opacification involving 20 lung regions as a surrogate for COVID-19 burden. We found that the CT-SS was higher in severe cases when compared with mild cases. Most importantly, we determined that a CT-SS threshold

of 19.5 could identify severe COVID-19, with a sensitivity of 83.3% and a specificity of 94%, resulting in a negative predictive value of 96.3%. Moreover, interreader agreement was excellent between our two radiologists. We envision that this relatively straightforward method could provide objective means to expedite the identification of patients with severe disease, especially in situations of limited availability of health care resources.

This retrospective study had several limitations. First, the CT-SS assumes that the amount of lung opacification is a surrogate for COVID-19 burden; however, there was no histologic confirmation of the findings. Second, we chose to analyze the first chest CT image obtained on admission; therefore, the studies were not controlled by the number of days since the start of symptoms, which could have potential implications for interpretation of the CT-SS. Indeed, our data show that patients in the severe group had a larger interval between the beginning of symptoms and hospital admission in comparison with patients in the mild group. Third, the CT-SS was only investigated within a small group (n = 2) of relatively experienced radiologists. Further research is needed to identify the degree of consistency of CT-SS among readers with different levels of experience. Finally, external validation studies with larger cohorts in multiple centers are still necessary to determine the validity of CT-SS and the proposed threshold before clinical translation.

In conclusion, this study provides a straightforward semiquantitative method for assessing severity of COVID-19 in the initial chest CT images. A CT-SS score less than 19.5 could rule out severe or critical forms of disease with a high negative predictive value of 96.3% in our cohort. CT-SS could be potentially used to expedite triage of patients in need of hospital admission. We envision that such an approach could be useful in scenarios combining high patient volumes and limited health care resources or polymerase chain reaction testing capabilities.

Acknowledgments: The authors thank Xinghua Liu, Yun Wen, Jingxian Xiong, Department of Radiology, Chongqing Three Gorges Central Hospital, for assisting with CT imaging data collection and Xu Wang, GE Healthcare, for assisting with statistical analysis of data.

Author contributions: Guarantors of integrity of entire study, all authors; study concepts/study design or data acquisition or data analysis/interpretation, all authors; manuscript drafting or manuscript revision for important intellectual content, all authors; approval of final version of submitted manuscript, all authors; agrees to ensure any questions related to the work are appropriately resolved, all authors; literature research, H.L.; clinical studies, R.Y., X.L., Y.Z., X.Z., Q.X., Y.L., C.G., W.Z.; statistical analysis, H.L.; and manuscript editing, H.L.

Disclosures of Conflicts of Interest: **R.Y.** disclosed no relevant relationships. **X.L.** disclosed no relevant relationships. **H.L.** disclosed no relevant relationships. **Y.Z.** disclosed no relevant relationships. **X.Z.** disclosed no relevant relationships. **Q.X.** disclosed no relevant relationships. **Y.L.** disclosed no relevant relationships. **C.G.** disclosed no relevant relationships. **W.Z.** disclosed no relevant relationships.

References

1. Gorbalenya AE, Baker SC, Baric RS, et al. Severe acute respiratory syndrome-related coronavirus: The species and its viruses – a statement of the Coronavirus Study Group. bioRxiv [preprint] https://www.biorxiv.org/content/10.1101/2020.02.07.937862v1.
2. World Health Organization. Novel coronavirus – China. Feb 11, 2020. https://www.who.int/docs/default-source/coronaviruse/situation-reports/20200211-sitrep-22-ncov.pdf?sfvrsn=fb6d49b1_2.
3. Zhu N, Zhang D, Wang W, et al. A Novel Coronavirus from patients with pneumonia in China, 2019. N Engl J Med 2020;382(8):727–733.
4. Zhou P, Yang XL, Wang XG, et al. Discovery of a novel coronavirus associated with the recent pneumonia outbreak in humans and its potential bat origin. bioRxiv [preprint]. https://www.biorxiv.org/content/10.1101/2020.01.22.914952v2.
5. Chan JF, Yuan S, Kok KH, et al. A familial cluster of pneumonia associated with the 2019 novel coronavirus indicating person-to-person transmission: a study of a family cluster. Lancet 2020;395(10223):514–523.
6. Lee N, Hui D, Wu A, et al. A major outbreak of severe acute respiratory syndrome in Hong Kong. N Engl J Med 2003;348(20):1986–1994.
7. Assiri A, Al-Tawfiq JA, Al-Rabeeah AA, et al. Epidemiological, demographic, and clinical characteristics of 47 cases of Middle East respiratory syndrome coronavirus disease from Saudi Arabia: a descriptive study. Lancet Infect Dis 2013;13(9):752–761.
8. Huang C, Wang Y, Li X, et al. Clinical features of patients infected with 2019 novel coronavirus in Wuhan, China. Lancet 2020;395(10223):497–506 [Published correction appears in Lancet 2020;395(10223):496.].
9. Koo HJ, Lim S, Choe J, Choi SH, Sung H, Do KH. Radiographic and CT Features of Viral Pneumonia. RadioGraphics 2018;38(3):719–739.
10. Pan Y, Guan H. Imaging changes in patients with 2019-nCov. Eur Radiol 2020 Feb 6 [Epub ahead of print].
11. Lei J, Li J, Li X, Qi X. CT Imaging of the 2019 Novel Coronavirus (2019-nCoV) Pneumonia. Radiology 2020;295(1):18.
12. Corman VM, Landt O, Kaiser M, et al. Detection of 2019 novel coronavirus (2019-nCoV) by real-time RT-PCR. Euro Surveill 2020;25(3).
13. General Office of National Health Commission. The Diagnosis and Treatment of Pneumonia Infected by Novel Coronavirus (5th Trial Edition). http://www.gov.cn/zhengce/zhengceku/2020-02/05/content_5474791.htm.
14. Chang YC, Yu CJ, Chang SC, et al. Pulmonary sequelae in convalescent patients after severe acute respiratory syndrome: evaluation with thin-section CT. Radiology 2005;236(3):1067–1075.
15. Li Q, Guan X, Wu P, et al. Early Transmission Dynamics in Wuhan, China, of Novel Coronavirus-Infected Pneumonia. N Engl J Med 2020 Jan 29 [Epub ahead of print].
16. Carlos WG, Dela Cruz CS, Cao B, Pasnick S, Jamil S. Novel Wuhan (2019-nCoV) Coronavirus. Am J Respir Crit Care Med 2020;201(4):P7–P8.
17. Xiao SY, Wu Y, Liu H. Evolving status of the 2019 novel coronavirus infection: Proposal of conventional serologic assays for disease diagnosis and infection monitoring. J Med Virol 2020;92(5):464–467.
18. Chinese Society of Radiology. Radiological Diagnosis of New Coronavirus Infected Pneumonitis: Expert Recommendation from the Chinese Society of Radiology (First edition). Chin J Radiol 2020;54:E001.
19. Paul NS, Roberts H, Butany J, et al. Radiologic pattern of disease in patients with severe acute respiratory syndrome: the Toronto experience. RadioGraphics 2004;24(2):553–563.
20. Ng MY, Lee EYP, Yang J, et al. Imaging profile of the COVID-19 infection: radiologic findings and literature review. Radiol Cardiothorac Imaging 2020;2(1):e200034.
21. Liu P, Tan XZ. 2019 Novel Coronavirus (2019-nCoV) Pneumonia. Radiology 2020;295(1):19.
22. Chung M, Bernheim A, Mei X, et al. CT imaging features of 2019 Novel Coronavirus (2019-nCoV). Radiology 2020;295(1):202–207.
23. Franquet T. Imaging of pulmonary viral pneumonia. Radiology 2011;260(1):18–39.
24. Song F, Shi N, Shan F, et al. Emerging 2019 Novel Coronavirus (2019-nCoV) pneumonia. Radiology 2020;295(1):210–217.
25. Wong KT, Antonio GE, Hui DS, et al. Severe acute respiratory syndrome: radiographic appearances and pattern of progression in 138 patients. Radiology 2003;228(2):401–406.
26. Ajlan AM, Ahyad RA, Jamjoom LG, Alharthy A, Madani TA. Middle East respiratory syndrome coronavirus (MERS-CoV) infection: chest CT findings. AJR Am J Roentgenol 2014;203(4):782–787.
27. Wu J, Wu X, Zeng W, et al. Chest CT Findings in Patients with Corona Virus Disease 2019 and its Relationship with Clinical Features. Invest Radiol 2020 Feb 21 [Epub ahead of print].